

Thermal Evolution of the Northeastern Siberian Platform in the Light of Apatite Fission-Track Dating of the Deep Drill Core

O. M. Rosen^a, A. V. Soloviev^a, and D. Z. Zhuravlev^b

^a *Geological Institute, Russian Academy of Sciences,
Moscow, Russia*

^b *Institute of Mineralogy, Geochemistry and Crystal Chemistry of Rare Elements,
Moscow, Russia*

Received December 11, 2008

Abstract—Thermal evolution of the continental crust beneath the northeastern Siberian craton was studied based on the interpretation of apatite fission-track ages. The samples selected for AFT dating were collected from depths between 2 and 3 km along a 1000-km-long profile, from the crystalline basement of the Siberian platform. The AFT ages range from 185 to 222 Ma, indicating that in the late Triassic–early Cretaceous, the top of the crystalline basement was cooled below $\sim 100^{\circ}\text{C}$. Once the apatite cooled below this temperature, it began to accumulate and preserve tracks produced by spontaneous fissioning of ^{238}U , and the number of tracks preserved is effective in determining the ages of events using the apatite fission-track method (AFT).

The study showed that the apatite from Archean rocks was largely formed at 1.8–1.9 Ga as a result of a Paleoproterozoic metamorphic overprinting during the terrane collision and the subsequent accretion of the Siberian craton. The last thermal event, the self-heating of the collision prism, was terminated by cooling at ~ 1.3 Ga. At that time, the Rb–Sr isotopic system became closed and the upper crust passed the $\sim 300^{\circ}\text{C}$ isograd. The calculation results showed that on further cooling, the $\sim 100^{\circ}\text{C}$ isograd was passed at 1143 Ma. This age estimate could be obtained using AFT dating if the above event had been the last one in the thermal history of the Siberian craton. The obtained track ages indicate the existence of a repeated, significantly younger, heating of the crystalline crust due to some local reason.

The present-day temperature at the sampling depth is 29°C based on the geothermal gradient curve, which was derived from the surface heat flow rate of 25 mW/m^2 and the crustal heat production value calculated from the concentrations of radioactive elements in the crust. In the near geological past, the maximum heat flow reaching 45 mW/m^2 was determined from the mineral equilibria in the mantle xenoliths from the 245–135 Ma kimberlites. Based on the respective geotherm, the crustal temperature in the study area did not exceed 53°C . It is obvious that an enhanced heat flux during kimberlite magmatism would not cause additional heating of the crust in the Mesozoic above $\sim 100^{\circ}\text{C}$.

The emplacement of flood basalts at 250 Ma was undoubtedly most important but underestimated the thermal event in the Mesozoic history of the Siberian platform. Numerous dolerite dykes were intruded at a great distance, far beyond the limits of the volcanic facies of the Putorana plateau, extending onto the study area. They were probably sourced from sills, which were emplaced along the base of the crust during basaltic underplating. The calculation results suggest that the reason of the crust's heating in the Mesozoic (222–185 Ma) might have been the emplacement of a large sill (or sills) into the base of the crust at 250 Ma. This heating of the top of the crystalline basement of the Siberian platform in the Mesozoic above $\sim 100^{\circ}\text{C}$ suggests that the respective heating event may have occurred at the base of the sedimentary cover and, thus may help in obtaining the age dates of the processes of the transformation of organic matter and oil generation.

PACS numbers: 91.35.Dc

DOI: 10.1134/S1069351309100085

INTRODUCTION

Fission-track dating enables the reconstruction of the thermal history of rocks. Apatite is often used to date the last cooling of the rocks below the closure temperature of about 100°C (AFT, apatite-fission-track method). In the northeastern Siberian craton, the last known thermal event, a self-heating of the collision prism, was terminated by cooling at ~ 1.3 Ga. At that

time, the Rb–Sr isotopic system became closed and the upper crust passed the $\sim 300^{\circ}\text{C}$ isograd [Rosen et al., 2006a]. Trap intrusion at about 250 Ma is likely to be another major thermal event; however, the data of variations in the crust temperature are generally unavailable. Therefore, the new apatite fission-track (AFT) data presented from the crystalline rocks help in understanding the thermal evolution of the Siberian Platform

and can be thus used in assessing the parameters of the formation of the oil pool.

Fission-track studies of apatites showed that they were formed, since the Archean, as individual mineral phases during the diachronous formation of metamorphic and granitoid rocks of the crystalline crust. At the same time, the observed AFT dates most probably represent the age of the last major thermal event in the history of the craton. This provides an excellent opportunity to study directly the thermal regime of the continental crust within the northeastern Siberian Platform.

LOCATION AND GEOLOGICAL SETTING OF THE STUDY AREA; SPECIFIC FEATURES OF THE ANALYZED SAMPLES

The study area is located in the northeast of the Siberian Platform, which comprises the Meso-Neoproterozoic (Riphean) and Phanerozoic platform cover, resting directly upon the crystalline basement forming the Siberian craton. The craton, with an area of some 4×10^6 km², is mostly overlain (70%) by sedimentary cover about 1–8 km thick (4 km on average). Phanerozoic foreland fold belts border the craton to the north and east, while it is bounded in the west and south by the Paleozoic and Mesozoic volcanic orogenic belts. The cratonic consolidated crust is a Paleoproterozoic collage of the Archean granulite-gneiss and granite-greenstone terranes of a different age, which were formed 3.5, 3.3, 3.0, and 2.5 Ga ago as independent microcontinents. Later, at 1.8–1.9 Ga after accretion they became amalgamated together through collision zones (sutures) [Rosen, 2004; Rosen et al., 2005; 2007], which are thought to be relics of paleoaccretion events [Parfenyuk, 2004; Parfenuk and Mareschal, 1997].

The granulite-gneiss terranes consist mainly of orthopyroxene plagiogneisses, enderbites (partly anatectites), two pyroxene mafic schists, (presumably island-arc meta-volcanites) and meta-carbonates and orthopyroxene quartzites, collectively belonging to the granulite metamorphic facies [Rosen, 2003]. These rocks are crumpled into narrow (few kilometers of the flank's width) isoclinal folds, which often make up large anti- and synforms and can be traced beneath the cover due to the intense positive linear magnetic (ΔT_a) and gravity signatures.

The granite-greenstone terranes comprising vast isometric, amoeboid-shaped granitoid bodies and linear folds, which have been squeezed in between them, are made up of mafic volcanites and greywackes (greenstone belts) or basite-ultrabasite metamorphosed to the greenschist and/or amphibolite facies and occupy about 10–20% of the area. This facies can be clearly distinguished beneath the sedimentary cover by its slight negative nonlinear mosaic magnetic and low gravity anomalies associated with large buried granitic plutons. However, the linear greenstone belts of various orienta-

tions and/or mafic-ultramafic intrusions have a strong positive magnetic signature.

Repeated episodes of deep cooling of the terrane's crust are documented by the first appearance of eroded areas, whose U–Pb ages obtained on the detrital zircons from quartzites and kinzigites (metapelites) were dated at 3.04, 3.0, 2.91, 2.58, and 2.56 Ga (see overview in [Rosen, 2004]).

The collision suture zones, which appear in their internal structure as a macroscale melange, represent the fracture zones along which terranes collided and joined (accreted or amalgamated). The melange consists of various blastomylonites and tectonites, migmatites, autochthonous granitoids and fragments of metamorphosed island-arc volcano-sedimentary rocks and large outliers of anorthozites and granulites from neighboring terranes. Varying in width from hundreds of m to 30 km, these outliers are clearly traceable beneath the cover for over 1000 km because they have a strong alternating linear magnetic signature.

During the initial stages, the terranes were accreted into large super-terrane or tectonic provinces (Fig. 1a), which later became constituent parts of the Siberian craton.

The Mesoarchean (3.2–2.8 Ga) in the evolution of the craton was marked by the development of sialic continental masses (proto-continents), which apparently underwent collision and accretion manifested at 2.8–2.6 Ga in regional granulite metamorphism and granite formation. All these proto-continents were presumably joined to form the supercontinent of Pangea-0, whose geologic features have not been yet revealed in the study area. Subsequently, this supercontinent broke up into several new microcontinents that apparently collided again in the late Paleoproterozoic, at 1.9–1.8 Ga. Microcontinents accreted into a collision prism were involved in granulite facies metamorphism and granite generation with subsequent transformation into tectonic blocks (terrane). This collisional structure was incorporated into a new supercontinent of Pangea-1, part of which constituted the Siberian craton in its present-day structure [Rosen et al., 2007].

The Olenek province is located in the northeast of the study area (Fig. 1b). Its western part comprises the Khapchan meta-carbonate-meta-greywacke sedimentogenic belt, which rests on the greenstone basement of the Birekta terrane. Further to the west, behind the Bilyakh suture the Anabar province, made up in its central part of the Daldyn granulite-gneiss terrane, is located. To the south, it adjoins the Markha granite-greenstone terrane overlain by the platform cover. The age and composition of the Markha terrane was determined from the core data and crustal inclusions in the kimberlites [Rosen et al., 2002; 2006a; Smelov et al., 1998]. Much farther to the west, the Magan granulite-gneiss terrane adjoins the two above the terrane along the Kotuykan suture.

In this area, a thickening of the crust of up to 58 km [Manakov, 1999] was probably inherited from the Paleoproterozoic collisional system. At the same time, this

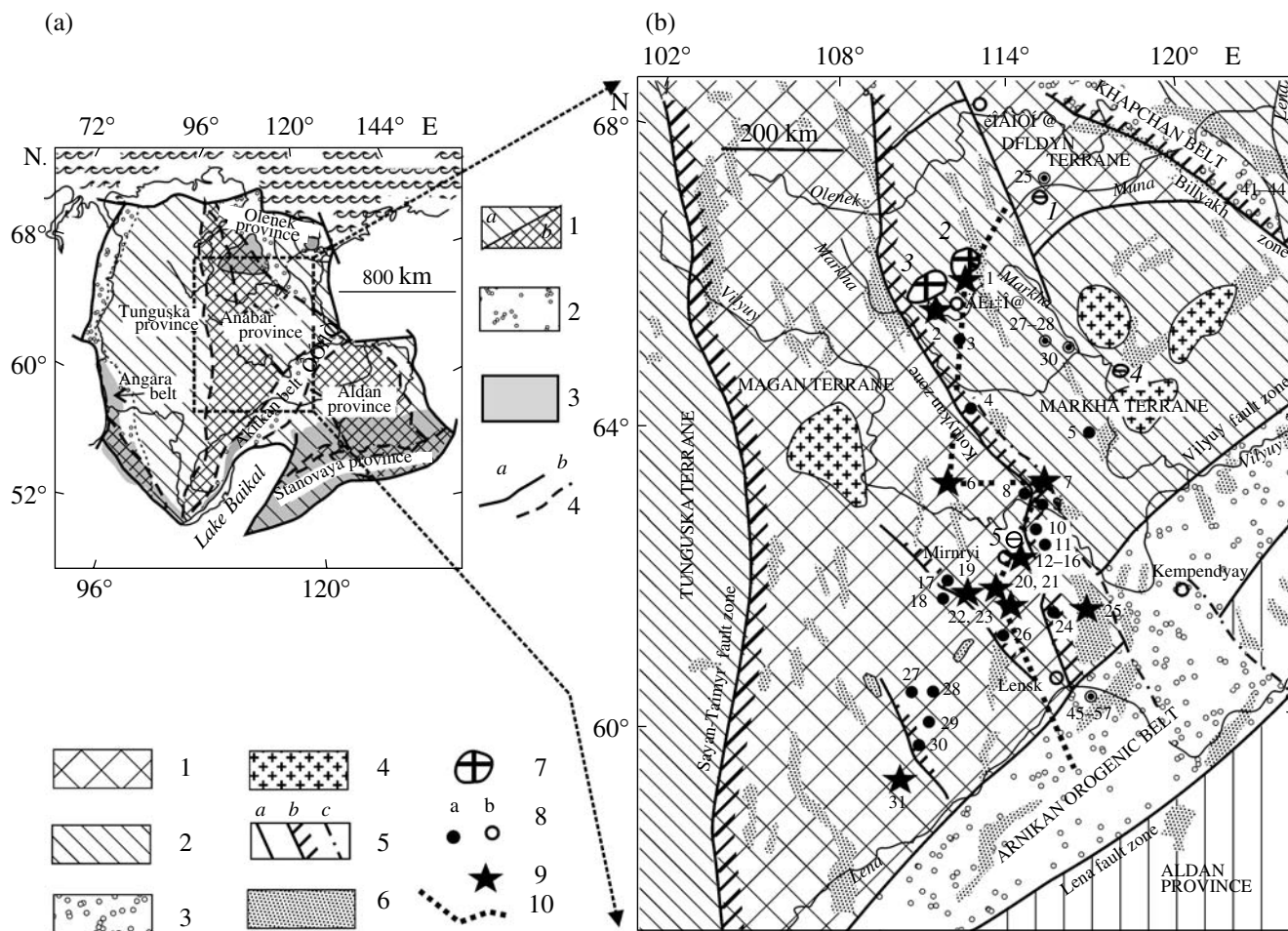


Fig. 1. Geological setting of the study area (after Rosen et al. (2002) and references herein.

(a)—Major tectonic elements of the Siberian craton.

1 – Archean terranes, 3.5–2.5 Ga, greenstone – *a*, granulite–gneiss–*b*; 2 – Proterozoic fold belts, 2.4–2.0 Ga; 3 – basement exposures; 4 – craton faulted boundaries – *a*, sutures within the craton – *b*.

(b) – Principal study area showing major structural features of the basement in the central part of the craton, kimberlite field and well locations: 1. granulite–gneiss terranes; 2. granite–greenstone terranes; 3. fold belts: metamorphosed volcanites, sediments, granitoids; 4. granite batholiths [Khoreva, 1987]; 5. Early Proterozoic sutures, *a*, *ibid.* NE-dipping overthrusts, *b*; 6. positive magnetic anomalies ΔT_a , over +5mE [Litvinova et al., 1978] reflecting the basement structure; 7. kimberlite fields: 1. Muna, 2. Daldyn, 3. Alakit, 4. Nakyn, 5. Mirnyi; 8. wells: *a* nos. 1–31 with a full section penetrated to the basement [Rosen et al., 2002]; *b*, numbers of individual samples from wells [Smelov et al., 1998]; 9. locations of samples used in this study for isotope geochronology [Rosen, 2006a; 2006b]; 10. schematic location of cross section, see also Fig. 3.

area is marked by an extensive positive gravity anomaly [Manakov, 1999], which is probably caused by the basalt underplating. The latter might be related either to the intrusion of mafites into the base of the lower crust during the collapse of a Paleoproterozoic collisional structure or the emplacement of dolerite sills during the Mesozoic trappean magmatism.

Core samples for this study were collected in wells 1, 6, 7, 20 (see Fig. 1b) from depths of 2000–3000 m. Detailed petrochemical and mineralogical data on each well shown in this figure are presented in Rosen et al. (2002). Core samples were taken at geologically significant intervals, typically from 2 to 70 m. The rocks samples are represented by amphibole and sillimanite gneisses and granite cataclasite (Table 1). The rocks are

felsic in composition: $\text{SiO}_2 = 63\text{--}66$ and 75; $\text{Al}_2\text{O}_3 = 14\text{--}17$, $\text{P}_2\text{O}_5 = 0.25\text{--}0.02$ wt % at $\text{Na}_2\text{O} > \text{K}_2\text{O}$, apart from the granite from well 7 where $\text{Na}_2\text{O} < \text{K}_2\text{O}$. The values of the Th/U ratios in gneisses from wells 1 and 20 are, respectively, 5.8 (typical of mature sedimentary rocks) and 2.3 (that is close to the values of the magmatic rocks). However, in other samples, this ratio reaches 21.7–24.7, which is probably indicative of the granulite depletion of the gneiss (well 6) and the partial melting of granite from the crust under high metamorphic conditions (well 7) (Table 2). This variation in chemical compositions of the rocks allows us to consider the fission-track ages as the representative temperature against time estimates for rocks from the Markha and Magan terranes.

Table 1. Sample location and mineral composition

Sample No.	Well No. 1*	Wellhead elevation, km	Wellhead elevation, km	Sampling depth, m	Sampling interval, m	Description**	Mineral composition***	Geological framework
Akh-703.2590	1	0.47	-2.12	2590	70	BiAm-gneiss	PlAmQB//Ti-MgtApZr//Ca	Markha terrane
BT-10.3008	6	1.34	-1.67	3008	5	CpxAmBi-gneiss	PlQKfsAmBiCpx//ApTi-Mgt//AmSrpCaGy	Magan terrane
S-1002.2703	7	0.27	-2.43	2703	25	Bi-granite cataclasite	PlQKfsBi//MgtAp//ChlMuCa	Kotuykan suture
100/2020	20	0.35	-1.67	2020	2	Sil2MicPl-gneiss	Q&lMusBiSil-Cord/ApZr//ChlTa	Magan terrane

Notes: * See Fig. 1.

** The positions for minerals are given in order of their increasing contents, e.g., CpxAmBi—the gneiss corresponds to a petrographic definition “clinopyroxene–amphibole–biotite gneiss.”

*** The positions of each mineral are given in order of decreasing contents and double slashed as follows: 1. rock-forming//, 2. accessory//, 3. secondary minerals (e.g., PlQB//ZrAp//ChlCa).

Petrographic symbols (international abbreviations after Siivola, Schmid (2007): Am, Ap, Bi, Ca, Chl, Cpx, Cord, Gy, Kfs, Pl, Q, Sil, Srp, ta, Ti-Mgt, Zr, 2Mic, are, respectively, amphibole (hornblend in most cases), apatite, biotite, carbonate, chlorite, clinopyroxene, cordierite, gypsum, K-feldspar, muscovite, plagioclase, quartz, sillimanite, serpentine, talc, titanium–magnetite, zircon, two–mica.

APATITE FISSION-TRACK DATING TECHNIQUE AND ANALYTICAL RESULTS

Apatite fission-track dating allows the reconstruction of the thermal history of rocks (e.g., [Wagner and Van der Haute, 1992]). Apatite grains accumulate linear trails of radiation damage to the crystal structure caused by the spontaneous fission of ^{238}U . Fission tracks in apatite are stable at relatively low temperatures, but at progressively higher temperatures, fission tracks become more annealed, until they are erased entirely. The temperature range over which annealing occurs is termed the *annealing zone*. The lower temperature limit of the annealing zone, at which 100% of tracks are stable, may cover a range of roughly 70°C, whereas the upper temperature limit, where tracks are unstable, is about 125°C (a heating duration of about 10 Ma). The effective closure temperature of apatite is estimated at $111 \pm 6^\circ\text{C}$ [Laslett et al., 1987]. Therefore, apatite can be used to estimate the time when the rocks last cooled below their closure temperature (about 100°C). Rock cooling may have occurred for a variety of reasons: cooling of intrusions after their emplacement, exhumation, and the exposure of rocks from depths at the closure isotherm of 100°C due to tectonic and isostatic movements.

It should be noted that the fission-track technique is now a widely used dating method with particular application to regional geological studies [Wagner and Van der Haute, 1992; Soloviev, 2008]. Below, we present

Table 2. Chemical composition of the studied samples

Sample No.	Akh-703.2590	BT-10.3008	S-1002.2703	100/2020
well No. 1*	1	6	7	20
SiO ₂	63.23	64.38	66.39	75.34
TiO ₂	0.58	0.48	0.35	0.14
Al ₂ O ₃	14.78	16.18	16.95	13.87
Fe ₂ O ₃ *	6.89	4.65	3.22	1.27
MnO	0.14	0.12	0.11	0.1
MgO	2.68	1.97	0.95	1
CaO	5.63	3.59	2.17	0.44
Na ₂ O	3.99	4.08	3.94	5.4
K ₂ O	0.89	3.12	4.68	1.49
P ₂ O ₅	0.16	0.25	0.13	0.02
LOI	0.99	1.15	1.08	0.89
Sum	99.98	99.97	99.98	99.98
Th	3.68	12.62	11.45	17.48
U	0.64	0.58	0.46	7.56
Th/U	5.78	21.7	24.71	2.31

Notes: * See Fig. 1.

** Total iron expressed as Fe₂O₃. XRF analyses of silicate rocks were performed at the laboratory of YaNIGP CNIGRI, ALROSA Co. Ltd., trace elements were determined by ICP-MS at the Institute of Mineralogy, Geochemistry and Crystal Chemistry of Rare Elements (IMGRE) under the guidance of D.Z. Zhuravlev.

Table 3. Apatite fission-track ages for drill core samples from the northeastern Siberian platform

Geological framework	Rock, sample No.	Mineral	ps	Ns	pi	Ni	pd	n	χ^2	Age	-1 σ	+1 σ	U \pm 2se
Markha terrane, well 1	Gneiss, 703/2590	Apatite	4.89	735	2.49	375	2.13	15	86.8	218.4	-16.0	+17.2	46.6 \pm 5.0
Magan terrane, well 6	Gneiss, 10/3008	Apatite	1.81	1296	1.08	771	2.11	20	95.4	185.9	-11.3	+12.0	20.4 \pm 1.6
Kotuykan suture, well 7	Granite, 1002/2703	Apatite	1.57	952	0.77	466	2.07	20	65.8	221.0	-15.1	+16.2	14.7 \pm 1.5
Magan terrane, well 20	Gneiss, 100/2002	Apatite	2.02	1159	9.92	569	2.09	20	47.9	222.6	-14.3	+18.9	9.8 \pm 1.0

Note: ps is the density of spontaneous tracks from ^{238}U ($\text{cm}^{-2} \times 10^6$), Ns is the number of tracks counted, pi is the density of the induced tracks from ^{238}U ($\text{cm}^{-2} \times 10^6$), pd is the density of tracks in the external detector (low uranium mica) ($\text{cm}^{-2} \times 10^6$), n is the number of grains counted, χ^2 is the chi-squared probability (%). A zeta calibration factor of 348.2 ± 11.02 (± 1 SE) for zircons was based on 8 age determinations (Fish Canyon Tuff and Buluk Tuff) [Hurford, 1998]. A Zeta factor of 106.33 ± 4.38 (± 1 SE) for apatites was based on 7 determinations (Fish Canyon Tuff and Buluk Tuff) [Hurford, 1998]. The samples were irradiated with thermal neutron flux of 8×10^{15} neutron/ cm^2 for apatite (Oregon State University reactor) simultaneously with the age standards and glass dosimeters with known U concentration (CN-1 for apatite). The tracks were counted at total magnification of 1562.5 X (dry) on an Olympus BH-P microscope fitted with an automated stage and a digitizing tablet. U is the uranium concentration in ppm (± 2 SE). All ages with $\chi^2 > 5\%$ are reported as pooled ages calculated using BinomFit v.1.8. [Brandon, 1996; 2002].

some examples of the application of the fission-track analysis in the study of ancient platforms or shields.

In Fennoscandia, the AFT ages reflect the topographic (altitude) distribution of crustal heating and cooling events. Relatively young AFT ages are characteristic of the mountain regions of Norway and Sweden, whereas the lowland depressions of Finland have older AFT ages [Hendriks et al., 2007]. For example, on the craton, the AFT ages range from 200 to 450 Ma in the most elevated parts of Sweden and 313–848 Ma in Finland [Murell, 2004]. The latter case records the earliest cooling ($T \leq 100^\circ\text{C}$) of 830–600 Ma and the Late Silurian heating event at 420 ± 20 Ma due to the development of the Caledonian foreland basin. The Cenozoic heating dates from central Sweden correspond to the age of the thermal metamorphism of coal at $T = 90$ – 220°C (vitrinite) and bitumen, which is observed westward, close to the eastern boundary of the Atlantic [Larson, 2006]. The hercynides from localities in Germany preserve a record of two heating events, one at 200 Ma related to the Triassic-Jurassic rifting in Europe, and another hydrothermal heating at 100 Ma during the early Alpine orogenesis [Jacobs and Breitzkreuz, 2003].

The map showing the distribution of AFT ages in Australia was compiled by Gleadow et al. [2002]. In Western Australia, the Pilbara and Yilgarn cratons preserve a signature of continuing slow cooling. In contrast, in the eastern part of the continent, including Tasmania, the AFT results record discrete episodes of rapid cooling during the Jurassic and Paleogene. Variations in the amount of denudation which the region has suffered over time scales of hundreds of Ma are assumed to be

the most likely reason of such regional variations in cooling ages.

In Canada, fission-track dating of the apatite samples from the 3440-m-deep well penetrated to the full section of the mafic Sudbury pluton, which intruded at 1.85 Ma [Lorenca et al., 2004], has yielded ages of 360 Ma at the wellhead and 140 Ma at the bottomhole. Such a spread of ages agrees with the geothermal gradient curve, which represents the increase of temperature with depth. The obtained age estimates are found to be unevenly distributed throughout the borehole section, follow a sinusoidal pattern, and stay between extreme values. This peculiarity can be explained by the degree of fission-track annealing, which is sensitive to apatite chemistry, particularly the chlorine content.

Thus, the AFT analysis, which enables recording the time a rock passes through the $\sim 100^\circ\text{C}$ isograd during cooling, can provide a powerful way to investigate geological objects, as is the case with the present study. Note that fission-track dates have not yet been obtained for all of the continents, and in Russia they have been used so far to decipher tectonic events that occurred on the convergent boundaries of the lithospheric plates during the Mesozoic-Cenozoic time [Soloviev, 2008]. Therefore, this study is the first attempt to examine the key factors that control mineral formation in the crystalline crust of the Siberian platform and reveal which types of thermal events may have caused the formation of apatite, then its subsequent metamorphic alteration and/or heating, and final cooling on passing through the $\sim 100^\circ\text{C}$ isograd.

The obtained results are given in Table 3 and Figure 2. In general, the apatite-fission track dating of rocks indi-

Table 4. Ages of the samples determined by different methods

Sample	Well	Sm–Nd		Rb–Sr		U–Pb zircon	AFT
		T ^{DM} 2st	MI	MI	IR		
Akh–703.2590	1			628 ± 39	0.7089 ± 4		218.4 ± 17.2
BT–10.3008	6	3100	1808 ± 54			2822	185.9 ± 12.0
S–1002.2703	7					2795 ± 6*	221.0 ± 16.2
100/2020	20			1783 ± 8.8	0.7226 ± 4	1876.1	222.6 ± 18.9

MI – mineral isochron.

IR – initial ratio.

* Discordia: 132 ± 14 and 2795 ± 6.

Source: Sm–Nd and Rb–Sr ages [Rosen et al., 2006a]; U–Pb ages [Rosen et al., 2006b]; AFT ages herein.

icates that cooling below 100°C occurred during the Late Triassic–Early Jurassic time (222.6 ± 18.9–185.9 ± 12.0 Ma). A huge area with a length of some 1700 km underwent cooling over this relatively short time span. The obtained age estimates should evidently represent a major geological event.

The other dating methods used confirmed that all the study samples are typical of the Siberian craton and the yielded geological ages represent the following successive events: magma extraction from the depleted mantle (3.0 Ga), granulite metamorphism (~2.8 Ga), collision-related formation of metamorphogenic deposits, and collision prism cooling (1.78–1.86 Ga up to 0.63 Ga) (Table 4). It is thus obvious that the AFT ages are not directly correlated with the ancient evolution of the craton but are likely to reflect a later thermal event (process).

Sample locations are shown in Figure 3. However, no correlation was found between the fission-track ages and hypsometric distribution of the study samples (Fig. 4). We speculate that the sample ages and age variability are not relief-dependent but may be for entirely endogenous reasons. In addition, the absence of a correlation between the concentrations of radioactive elements in the study rocks and their fission-track ages (Fig. 5) directly indicates that the obtained age estimates are dependent on the accumulation of fission tracks in apatite over geologic timescale rather than the overall geochemical variability of the rocks. Based on petrochemical data, the rocks studied are close in their composition to the rocks from the middle crust (Fig. 6), which is consistent with the sample locations within sections and thought to be indicative of the depth and directly indicates the deep erosion of the craton owing to which the upper, mainly granite, crust has been largely eroded prior to accumulation of the Riphean-

Phanerozoic cover [Rosen, Fedorovskii, 2001] and washed out to the surrounding catchment basins.

THERMAL HISTORY OF THE NORTHEASTERN SIBERIAN CRATON

Natural apatites used in the AFT analysis were formed, since the Archean, as individual mineral phases during the diachronous magmatic and metamorphic rock formation events as well as during the formation of anatectite granitoids. The apatites are known to retain and accumulate fission tracks, until they become annealed at temperatures over ~100°C. Therefore, a correct assessment of any circumstantial evidence in the dating of samples will require a thorough consideration of major thermal events in the history of the northeastern part of the Siberian craton (Table 5).

The earliest event in the geologic history of the continental crust is the formation of the TTG (tonalite–trondjemite–granodiorite) suite or the so-called grey gneisses. TTG suites are generally found on the Siberian craton as well as over other cratons, or within the cratonic cores formed mainly at 3.2–3.6 Ma, in the Paleoproterozoic erathem (see overview in Rosen and Schipanskii [2007]). Tonalite is believed to have been produced by the partial melting of subducted mafic crust under conditions of gentle (or hot) subduction, ascending to the top, and being segregated into trondjemite and granodiorite to form primary sialic crust [Martin and Moyen, 2002]. The TTG suite underwent anatexis under conditions of granulite facies, which generated autochthonous enderbites and granitoids. This seems to be the way the primary continental masses, i.e. microcontinents, originated to subsequently form parts of the Siberian craton [Rosen and Turkina, 2007]. This was followed by a delayed process of island-arc formation that could be rather widespread.

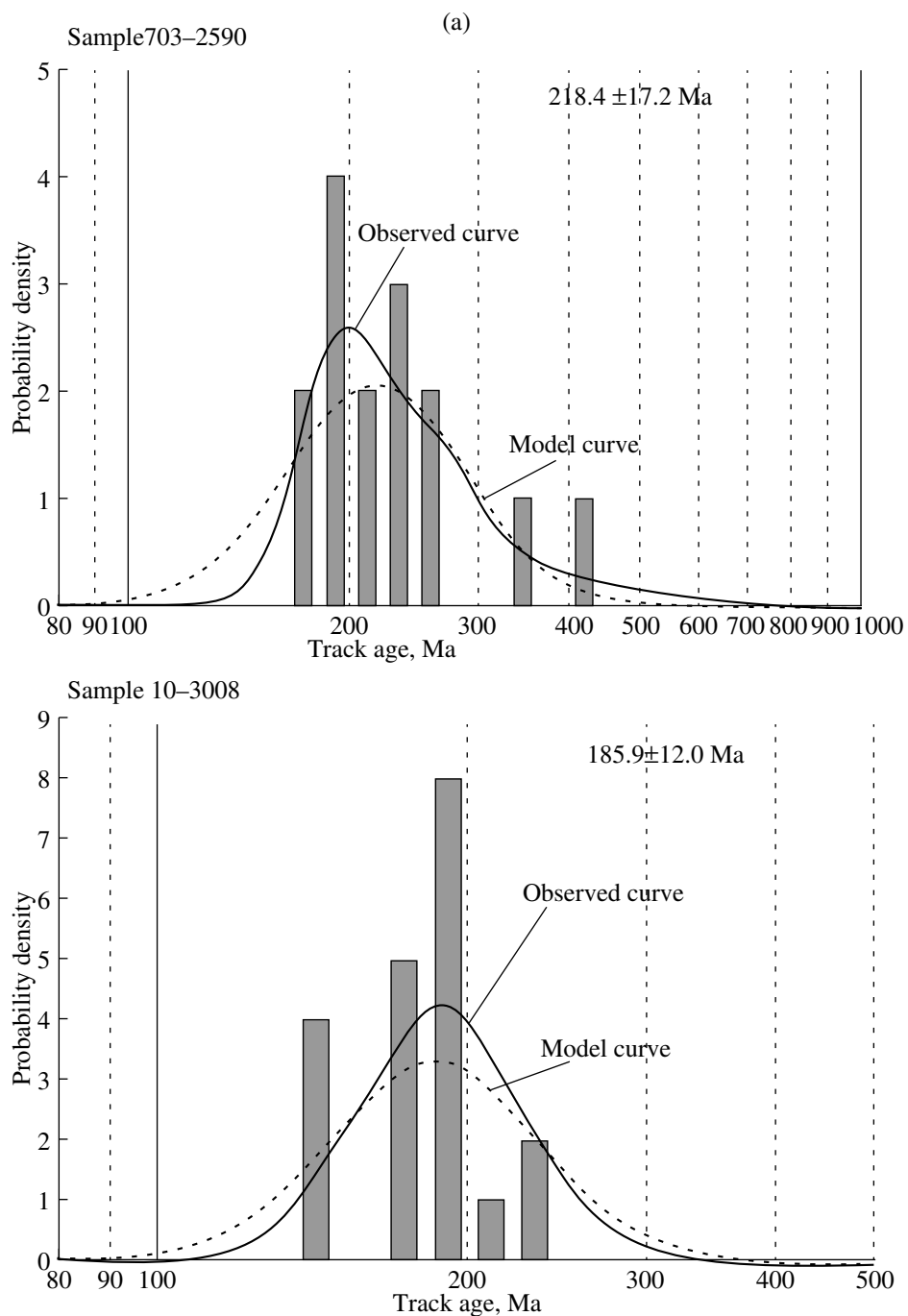


Fig. 2 (a) The AFT age distribution in samples from well 1 (sample 703-2590) and well 6 (sample 10.3008); (b) The AFT age distribution in samples from well 7 (sample 1002-2703) and well 20 (sample 1100-2002).

These two sources appear to have supplied the major portion of the sialic crust material of the primary microcontinents, which were later transformed into granulite-gneiss terranes. Since 2.9 Ga, island arcs also supplied the source materials for greenstone belts. Greenstone belt development terminated with the 2.3 Ga granite-forming event, which was intense and profound in its regional extent. This probably also marks the ter-

mination of the formation of the primary granite-greenstone microcontinents (the subsequent terranes).

The next, most distinctive stage was manifested largely as an accretion of microcontinents, their welding by collision into terranes, which make up the present-day framework of the Siberian craton. A comparison of the model and isochron ages of these processes is given

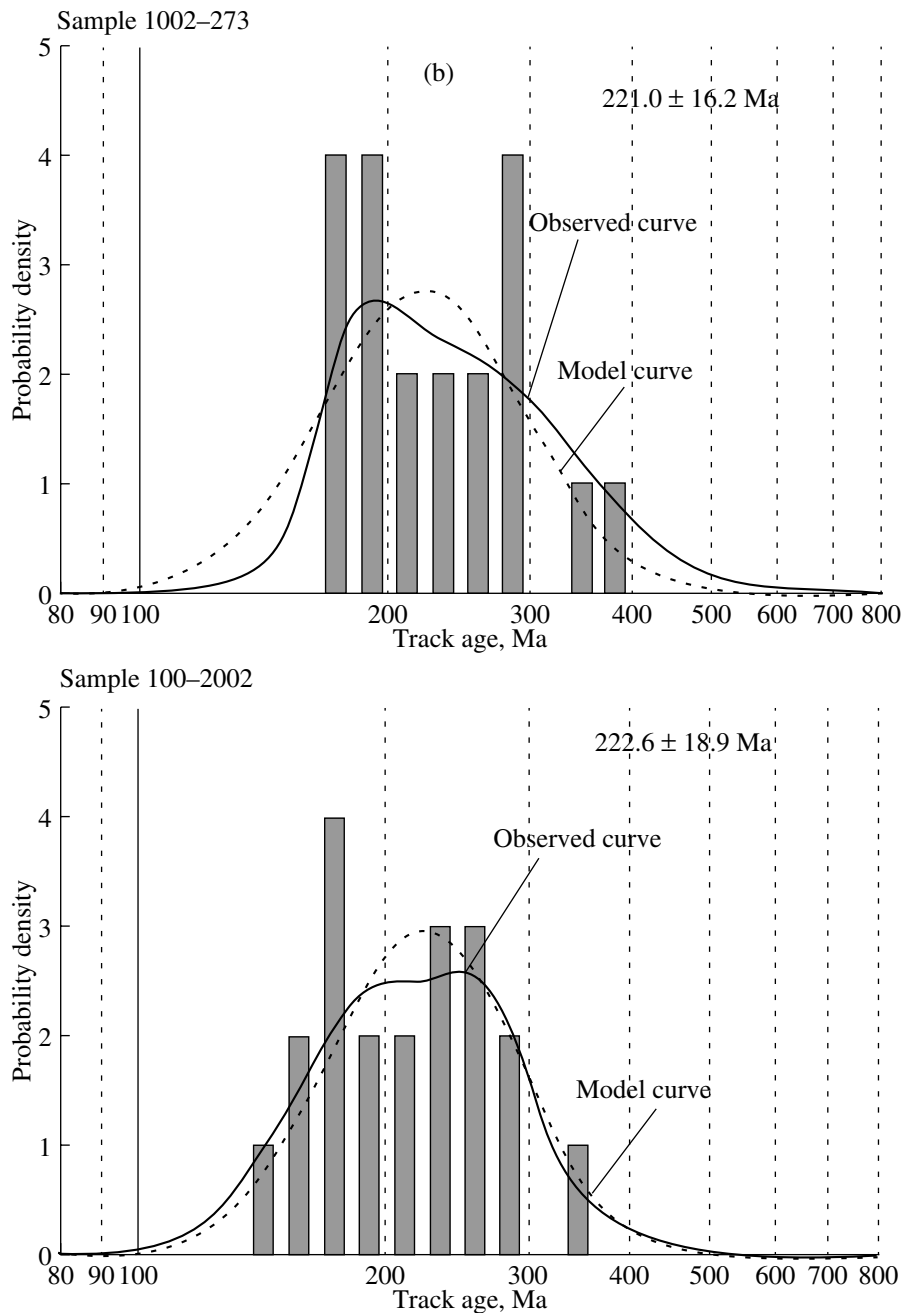


Fig. 2. Contd.

in Fig. 7. Stepwise heating simultaneously affected the 2.9–3.3 Ga and 2.3–2.9 Ga terranes, which were parts of a single collision prism. This episode terminated 1630 Ma ago and was initiated as a granulite metamorphism overprinting the primary rocks and anatectic generation of the granitoids by partial melting. The Sm–Nd mineral isochrones were obtained for garnet granulite facies rocks, containing apatite as a single phosphate phase. These isochrones are thus interpreted

to reflect the widespread development of apatite, which was, in particular, successfully analyzed in this study using the fission-track method. Subsequently, the collision prism underwent cooling to the temperature of 300°C at which the biotite Rb–Sr system equilibrated (Fig. 8a). These biotite Rb–Sr ages were found to demonstrate a systematic time lag (Fig. 8b). This time lag was calculated based on the mineral isochron results obtained for the same sample by the equation $(Rb-Sr) = 0.8 (Sm-Nd)$ given the

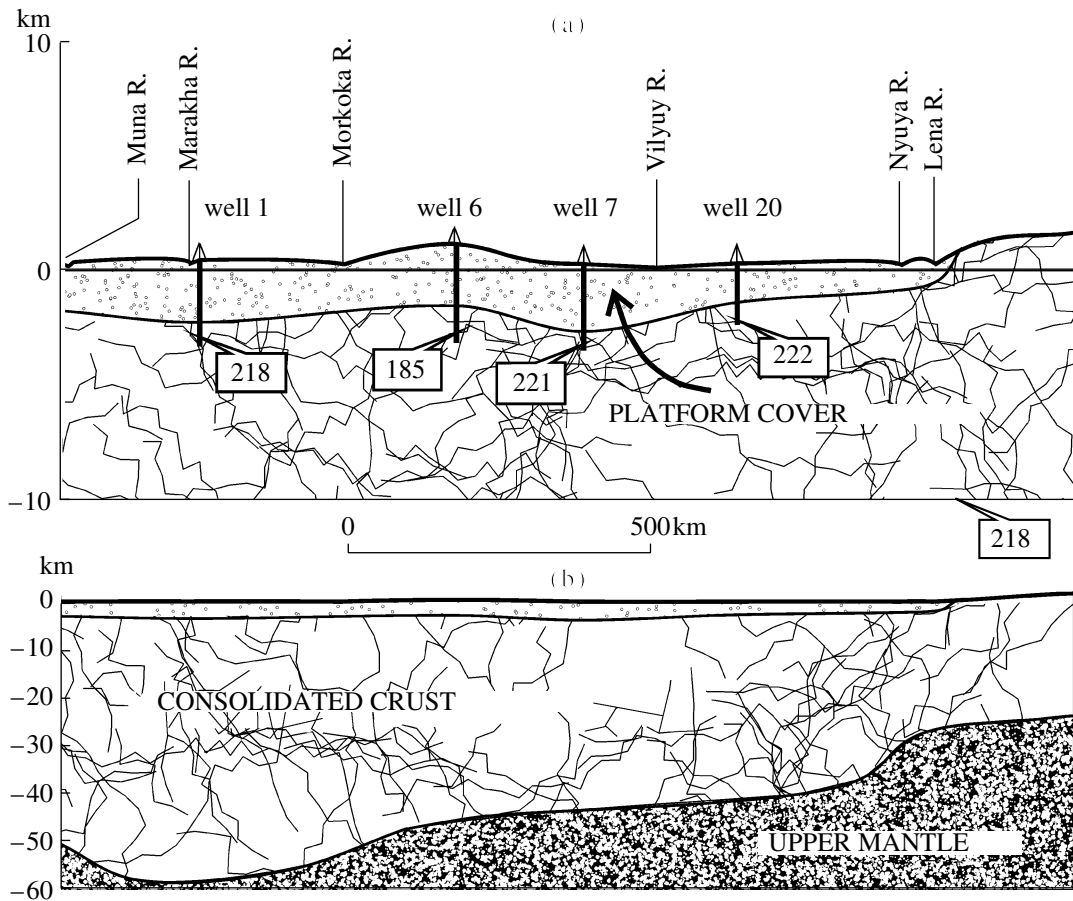


Fig. 3. Location of dated samples along the line Muna R. to Lena R.

(a) Cross section through the upper crust to a depth of 10 km; (b) Full section of the crust (after Rosen et al. [2005]; 1. apatite fission-track ages. The location of the cross section is shown in Fig. 1.

validity of approximation of $R^2 = 0.86$ (Fig. 8c), which corresponds to a correlation coefficient of 0.93. Such a dependence allows us to interpret the Rb-Sr dating results as geochronologically meaningful data. It means that a collision-related thermal event was terminated in the region at 1300 Ma (or partially later) with a temperature of 300°C. This indicates that the complete recrystallization of the granulite-amphibolite facies rocks due to collision-related metamorphism and the formation of apatite were terminated by the early Mesoproterozoic (1.6 Ga).

Could it be the last heating event after which apatites were gradually cooled to ~100°C up to the Mesozoic? It can readily be verified. Based on the Sm-Nd garnet-mineral isochron data, a collision-related metamorphic event was terminated at 1600 Ma with a temperature of ~700°C (see Fig. 8a). While the Rb-Sr biotite system records a cooling to 300°C at 1300 Ma. Then the cooling rate can be calculated as $(700-300^\circ\text{C})/(1600-1300)\text{ Ma} = 1.3^\circ\text{C/Myr}$. Then the cooling from 300°C to 100°C spanned over a period of

153 Ma, and this cooling episode had a duration from 1300 until $(1300-153) = 1143\text{ Ma}$. It means that the collisional system probably passed through the ~100°C isograd during the Late Mesoproterozoic, i.e., some 1 Ga prior to the event dated in this study by the fission-track method. It is obvious that over this long geological time span there was an episode of reheating followed by a new cooling event. This double event was reflected in our AFT dating results.

We have now to look for the age and the causes of this reheating event. The AFT age estimates seem to be affected by endogenous processes related to kimberlite emplacement and intrusion of the flood basalts. Indeed, the overall volume of kimberlite diatremes is insignificant compared to the volume of the crust in the region. Although the kimberlite emplacement had not caused the increased heating of the crust's interior and the annealing of the fission track in the apatites, the enhanced heat flow during kimberlite magmatism may have led to significant crustal heat production at 344–360 Ma in the Paleozoic, during the intense kimberlite

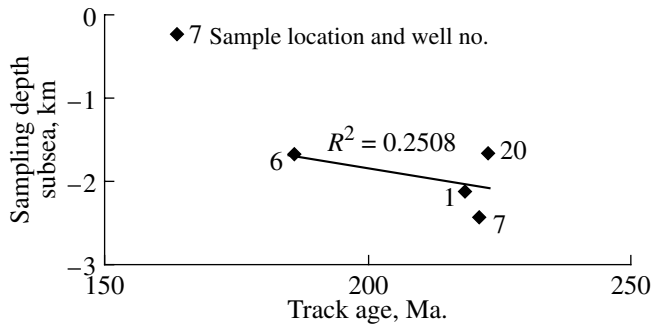


Fig. 4. A plot of the AFT ages against sampling depth subsea. R^2 is the reliability factor corresponding to the correlation coefficient $R = 0.5007$, insignificant relationship.

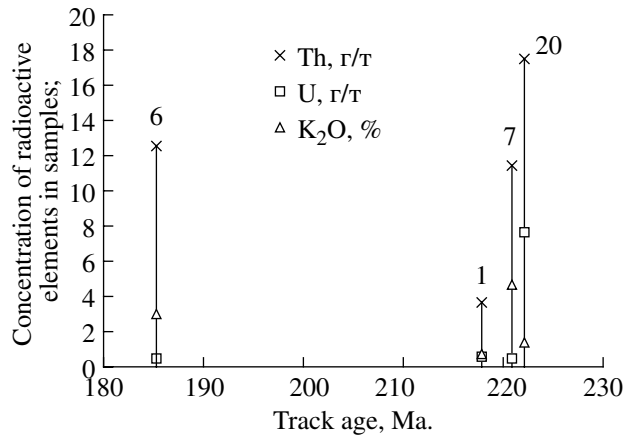


Fig. 5. A plot of apatite fission track ages against concentrations of radioactive elements in samples.

emplacement episodes, and at 245–135 Ma in the Mesozoic (Fig. 9).

The emplacement of flood basalts of the trappean formation at 250 Ma certainly had a significant yet poorly studied thermal effect. This was greatly added by the widespread development of dykes and sills

around the volcanic field. All the cored wells are located within the area of scattered intrusions, on the interfluvium between the Vilyuy and Olenok rivers (Fig. 10). We suppose that the obtained AFT age estimates were somehow related to a trappean event which occurred at the Permian-Triassic boundary.

Table 5. Thermal history of the northeastern Siberian craton

Age	$T, ^\circ\text{C}$	Process	Source
Age, Ga			
3.2–3.4	1000–1050*	Formation of primary crust, production TTG grey gneisses via melting of basaltic oceanic crust	[Rosen, Turkina, 2007]
2.9–3.1	950–1000*	Formation of the initial island–arc substrate of granulite–gneiss terranes	[Vishnevskii, 1988; Rosen et al., 2006b]
2.9–2.4	800–950*	Melting of granitoids in granite–greenstone terranes	"
1.7–2.2	850–1050*	Collision of microcontinents (terranes) and accretion of the Siberian craton	"
1.8–1.3	300–850*	Cooling of the collision prism	[Rosen et al., 2006b]
1.2	1000–1100**	Ingashi kimberlite field, southwest of the Siberian craton	[Rosen et al., 2008]
Age, Ma			
344–360	1000–1100** 35 mW/m ² ***	Kimberlite fields in the east of the craton – Mirnyi, Alakit, Daldyn etc.	[Rosen et al., 2008]
250	900–1320**	Flood basalts in the west and center of the craton, alkaline ultramafic complexes with carbonatites in the northeast of the craton	"
245–135	1000–1100** 40–45 mW/m ² ***	Kimberlite fields in the northeast of the craton: Kharamay, Verkhnyaya Kuonamka, Kuranakh, Kuoyka etc.	"
0	29–285* 25 mW/m ² ****	Steady–state conditions on the Anabar shield	[Rosen et al., 1992]

Notes: * Areal temperature of the crust.

** Temperature of the magmatic body during emplacement.

*** Heat flow rate calculated from mineral thermobarometers for mantle xenoliths from kimberlites [Griffin et al., 1996; 1999; Ashchepkov et al., 2007].

**** Direct observations [Duchkov et al., 1982].

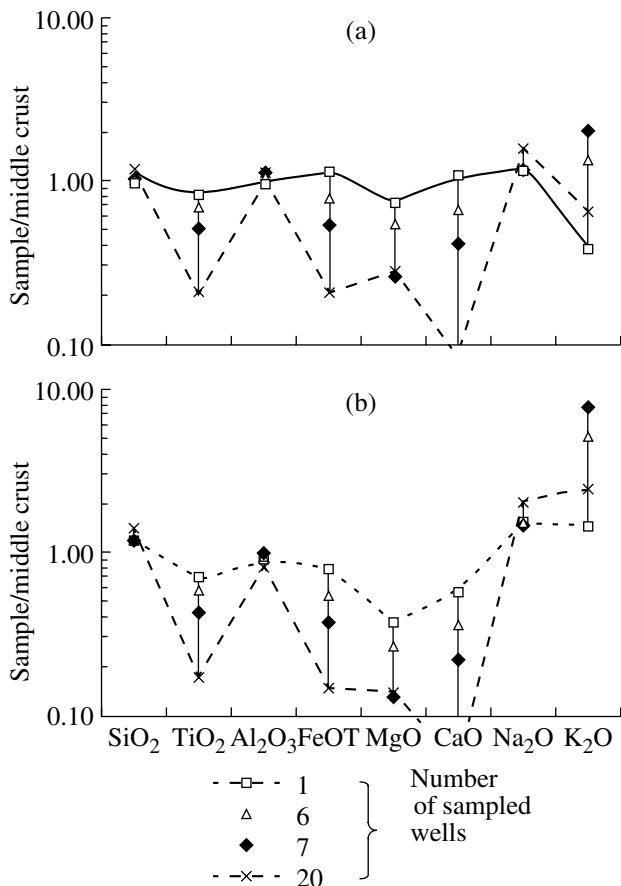


Fig. 6. Chemical composition of samples against average composition of the crust [Rudnick and Gao, 2003]. Comparison with the middle crust composition (a) and lower crust composition (b).

THERMAL REGIME OF THE NORTHEASTERN SIBERIAN CRATON

The measured surface heat flow ($Q_0 = 25 \text{ mW/m}^2$) for the northern framing of the Anabar shield [Duchkov et al., 1982] is close to the mean heat flow values ($\sim 27 \text{ mW/m}^2$) in the eastern Siberian platform (Yakutian kimberlite province) [Duchkov and Sokolova, 1997]. These heat flow values are lower than the present-day values of ($46\text{--}54 \text{ mW/m}^2$) measured on the other diamond-bearing platforms. During kimberlite magmatism, heat flow values were moderate and almost identical in the lithosphere of all kimberlite provinces (including Yakutia), ranging between 35 and 47 mW/m^2 (determined from mantle xenolith thermobarometry) [Duchkov and Sokolova, 2005]. To facilitate the reconstructions, we consider in the following near-real simplified parameters: the crustal thickness is $\sim 40 \text{ km}$, the sampling depth is $\sim 3 \text{ km}$, and the AFT age is $\sim 220 \text{ Ma}$.

The heat production rate within the shield crust (thickness weighted average, $Z = \sim 40 \text{ km}$) is estimated

to be $A = 0.36 \mu\text{W/m}^3$, varying from 0.76 in the upper crust to 0.076 in the lower crust and up to 1.22 in local migmatite–tectonites of the collision zone [Rosen, 1992]. Such low values may be caused by a deficit of heat-producing radioactive elements. The granitic upper crust, the major source of radioactive elements, is assumed to have been eroded as a result of the washing out of the Proterozoic collision-related mountain structure [Rosen and Fedorovskii, 2001].

The crustal component of heat flow in this region is determined as $Q_c = A \mu\text{W/m}^3 \cdot Z \text{ km} = 14.2 \text{ mW/m}^2$. In this case, the mantle component will be defined as $Q_m = Q_0 - Q_c = 10.8 \text{ mW/m}^2$, or 43% of the surface heat flow. This is an abnormally low contribution because the cratonic heat flow usually demonstrates an inverse ratio of (0.4 to 0.6) [Pollack and Chapman, 1977], although recent estimates for the regions with an Archean crust reflect an increasing crustal component up to $52\text{--}85\%$ of the overall heat value [Rudnick and Fountain, 1995].

At a depth of 40 km (approximately at the base of the crust), the temperature (T_z) calculated by the formula from Rosen and Milanovskii [1988]

$$T_z = T_0 + Q_0 \cdot Z/\lambda - A \cdot Z^2/2\lambda$$

where $T_0 = 0^\circ\text{C}$ is the earth's surface temperature, and $\lambda = 2.5 \text{ W m K}^{-1}$ is the thermal conductivity, will be equal to 285°C [Rosen, 1992]. The calculated paleotemperature and mantle heat flow are close to the results [Duchkov and Sokolova, 1985; 1997] of direct observations of the surface heat flow ($10\text{--}12 \text{ mW/m}^2$) and the temperature at the base of the crust ($200\text{--}300^\circ\text{C}$). This temperature is markedly lower than the mean values measured for the ancient shields ($350\text{--}400^\circ\text{C}$) (Fig. 11), Meso–Cenozoic orogens ($500\text{--}600^\circ\text{C}$), and Cenozoic rift systems ($650\text{--}750^\circ\text{C}$) [Condie, 1989]. The geodynamic reconstructions for the base of the mature continental crust are often based on the temperature value of $\sim 560^\circ\text{C}$, e.g. 556°C [Jamieson et al., 1998] or 567°C [England and Thompson, 1984].

During the emplacement of the kimberlite, the average heat flow in the region was significantly higher than the present-day values, equal to $35\text{--}45 \text{ mW/m}^2$, as suggested by the conductive model calculated garnet [Griffin et al., 1996; 1999] and pyroxene [Ashchepkov et al., 2007] thermobarometry of the mantle xenoliths. Two types of xenoliths are usually recognizable within one kimberlite field. The first type of xenoliths are coarse-grained, low-temperature ($900\text{--}1000^\circ\text{C}$), falling on a $35\text{--}40 \text{ mW/m}^2$ geotherm and presumably reflecting the sub-continental lithosphere. At the same time, fine-grained, often cataclased, high-temperature ($\sim 1100\text{--}1200^\circ\text{C}$) xenoliths fall on a $40\text{--}45 \text{ mW/m}^2$ geotherm. This corresponds to a local short-term heating episode

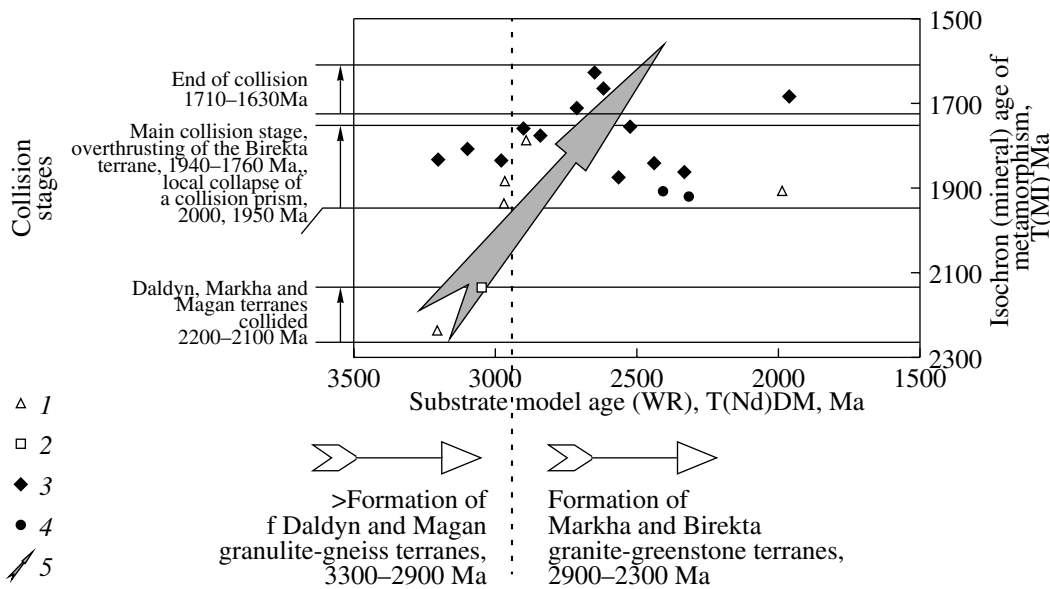


Fig. 7. A relationship between the model Sm–Nd (WR) and mineral isochron ages [Rosen, 2006a], partially confirmed by U–Pb zircon dating [Rosen, 2006b].

1–4, terranes where samples have been collected: 1. Daldyn, 2. Magan, 3. Markha, 4. Birekta, 5. age trend of collision-related metamorphisms.

caused by emplacement of an intrusion and a perturbation of the conductive geotherm at the base of the lithosphere, which marks the lithosphere–asthenosphere boundary [Griffin et al., 1996; 1999].

In Late Paleozoic kimberlite fields [Mir, Alakit, Daldyn - 360 Ma, Muna – 344 Ma; see age estimates in Rosen [2000]), xenoliths unaffected by a thermal anomaly in the asthenosphere define a 35 m W/m² geotherm with the xenolith recrystallization temperature of ~900–1100°C [Griffin et al., 1996; 1999]. The temperature estimated at the base of the crust, at a depth of 40 km, was equal to 445°C. Mesozoic kimberlite fields (Kuoyka, Kuranakh, Luchakan, and others, 245–135 Ma [Rosen, 2000]) carry xenoliths that were metamorphosed to a 40 m W/m² geotherm at the temperature of up to 1000°C [Griffin et al., 1999], which corresponds to the crustal temperature of 525°C at a depth of 40 km. Assuming a maximum possible geotherm of 45 mW/m², the maximum crustal paleotemperature is estimated to be 605°C at a depth of 40 km.

Heat flow values calculated from xenolith petrology suggest that temperatures near the crustal base reached 445°C in the Late Paleozoic, and 525°C in the Mesozoic, given the maximum possible value of 605°C. These paleotemperatures fall within the range of those considered characteristic of a mature continental crust. During the Cenozoic, heat flow drastically decreased, and the temperature at the base of the crust was as low as 285°C. Such an unusually low value is interpreted to be a natural anomaly. It is assumed that a generally low

heat flow in the Cenozoic may have caused the development of permafrost at ultra-deep levels within the crust of the Siberian platform [Duchkov and Sokolova, 2005]. The calculated geothermal gradients suggest that the subsurface temperature at a depth of 3 km is presently 29°C, and reached its maximum value of 53°C during the emplacement of the kimberlite (Fig. 12). Thus, the intrusion of the kimberlites themselves could not generate enough heat to completely anneal the tracks in the apatites (~100°C). Therefore, these thermal events could not be reflected in the apatite fission–tracks' apparent ages.

CAUSES OF THE CRUSTAL REHEATING

Flood basalt magmatism at 250 ± 2 Ma [Dalrymple et al., 1995; Renne and Basu, 1991] caused the emplacement of numerous veins and minor dolerite sills, which spread wide and far beyond the tuffaceous volcanic units and the Norilsk magmatic field. The distance from the plume feeder conduit is some 500–1000 km (see Fig. 10). The dolerite dykes and sills mapped at the surface often make up a significant portion of intruded rocks. For example, within the Anabar shield they constitute sometimes 15–20% of the exposed surface, with individual bodies ranging in thickness from 50 to 200 m, rarely more, and 1–20 km long [Rosen et al., 1986]. Since these dykes do not display any preferred orientation they cannot be taken as indicating the location of the plume feeder, as reported in recent publications

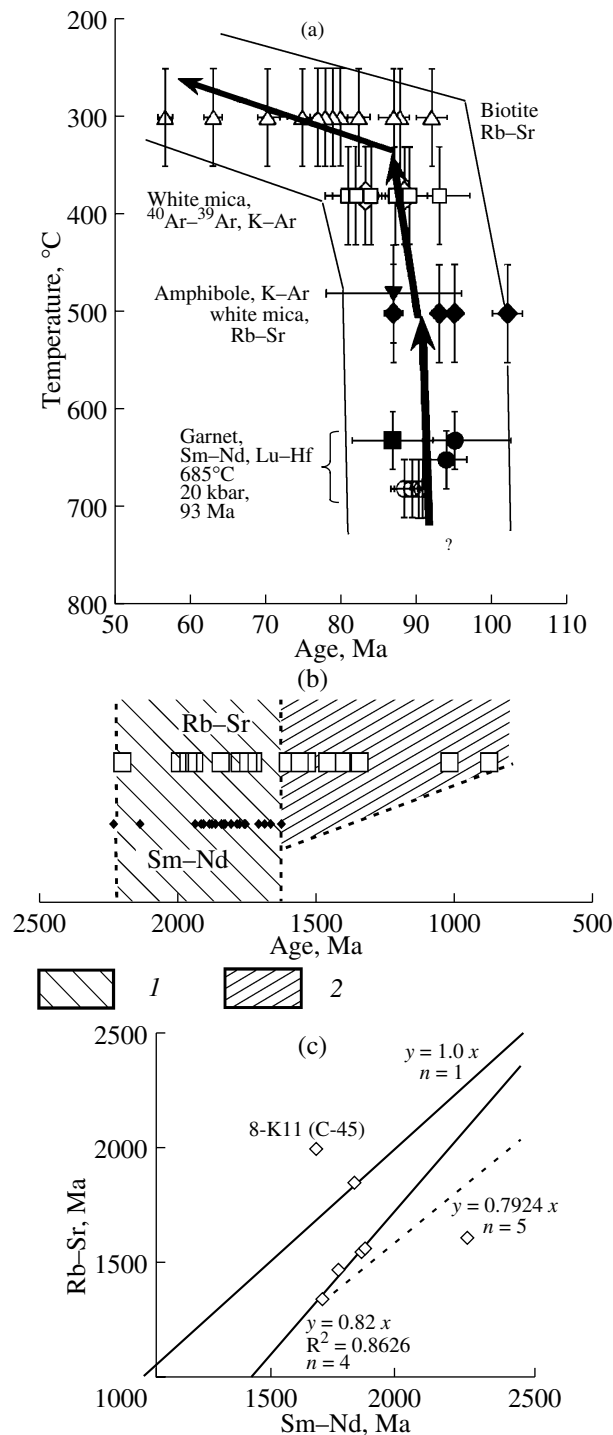


Fig. 8. A relationship between Rb-Sr and Sm-Nd mineral isochron ages and their thermal interpretation.

(a) Temperature–time relation of isotope equilibrium in minerals from the collision prism [Thöni, 2003]; (b) composite Rb-Sr and Sm-Nd diagram: 1. area of concordant ages, 2. area of decreased Rb-Sr ages; (c) comparison of Rb-Sr and Sm-Nd ages obtained for the same samples. Errors are less than the size of the symbols plotted.

[Dobretsov, 1997; Dobretsov et al., 2006; Fedorenko et al., 1996]. In other words, there is no radial dyke swarm within the upper crust of the Siberian platform, which could, as in many other flood basalt provinces, directly

indicate the path the magma follows away from the plume feeder. In the study area, the magma may have been supplied to dyke complexes from deeper levels in the lower crust, then spread horizontally at the same depths, moving

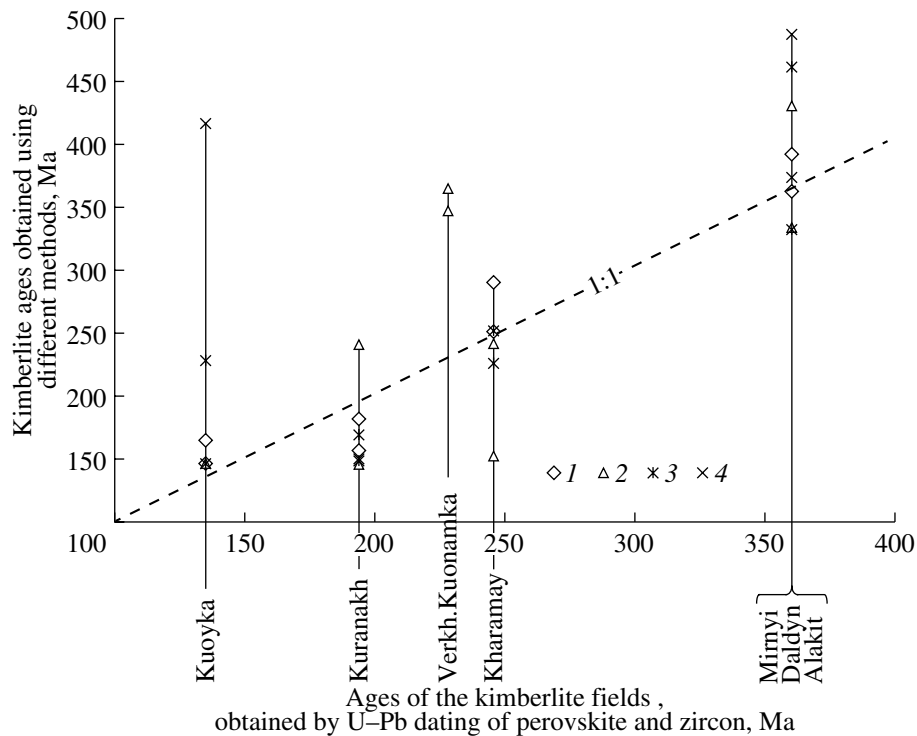


Fig. 9. Age dates for the kimberlite fields based on the kimberlite pipe ages obtained using different isotopic dating systems, including the U–Pb dating of perovskite [Kinney et al., 1997] and zircon [Devis et al., 1980]:

1—4, ages of the kimberlite emplacement determined by: 1. zircon fission-track (ZFT) analysis; 2. Rb–Sr; 3. K–Ar; 4. ³⁹Ar–⁴⁰Ar (data presented in Rosen [2000]).

away from the plume over a large distance. The proposed magma transport path is most favored for the crust-mantle boundary, and the process itself can be interpreted as basaltic underplating.

To calculate the thermal impact of the basaltic underplating at various crustal levels, we used the most probable temperature of 1320°C, indicating basalt injection into the lower crust [Bohrson and Spera, 2001]. The energy consumed during exocontacts alterations, such as high temperature hornfelsing, can be neglected. Geotherm 5 (Fig. 12) implies that a temperature of 107°C at a depth of 3 km, where the dated samples were collected was sufficient to initiate track annealing in apatites. It is obvious that upon sill injection, it might take a certain time interval for the heat to penetrate through the crust and an equilibrium geotherm to be attained.

We calculate the timing of thermal equilibration in the crust after the underplating event and the establishment of an equilibrium geotherm by the formula of E.V. Artyushkov (1993) applied for evaluating the time of thermal diffusion in the lithosphere in response to a perturbation:

$$\tau \sim h^2/(\pi^2 \chi),$$

where τ is the diffusion time, Ma, h is the layer thickness, 40 km in our case, $\pi = 3.14$, and χ is the thermal diffusivity taken as $\sim 0.01 \text{ cm}^2/\text{s}$ [Aryushkov, 1993] out of a possible 0.005–0.025. The calculation results show that at the specified conditions the duration of the thermal diffusion through the crustal profile should be $\tau = 5.15 \text{ Ma}$. By the end of this time interval, the temperature in the crustal profile should correspond to the calculated equilibrium geotherm 5 (Fig. 12). Then, if the underplating occurred at 250 Ma, the equilibrium must have been attained 244.85 Ma ago, followed by a period of cooling. Cooling to $\sim 100^\circ\text{C}$ at a depth of 3 km probably took 24.85 Ma, since the AFT age for this temperature was estimated at $\sim 220 \text{ Ma}$. Thus, it was reasonably assumed that after the sill was emplaced into the crust base (250 Ma) and the thermal equilibrium by diffusion was attained in the crust (244.85 Ma), another 24.85 Ma must have passed until the temperature at the sampling depth decreased below the $\sim 100^\circ\text{C}$ isotherm and the apatites began to accumulate fission tracks, which enabled us to obtain an age of $\sim 220 \text{ Ma}$.

In general, Mesozoic apatite fission-track ages for the crystalline basement of the Siberian platform are most likely to record crustal heating induced by the basaltic underplating during basalt eruption at 250 Ma and the subsequent cooling episode. The variations in

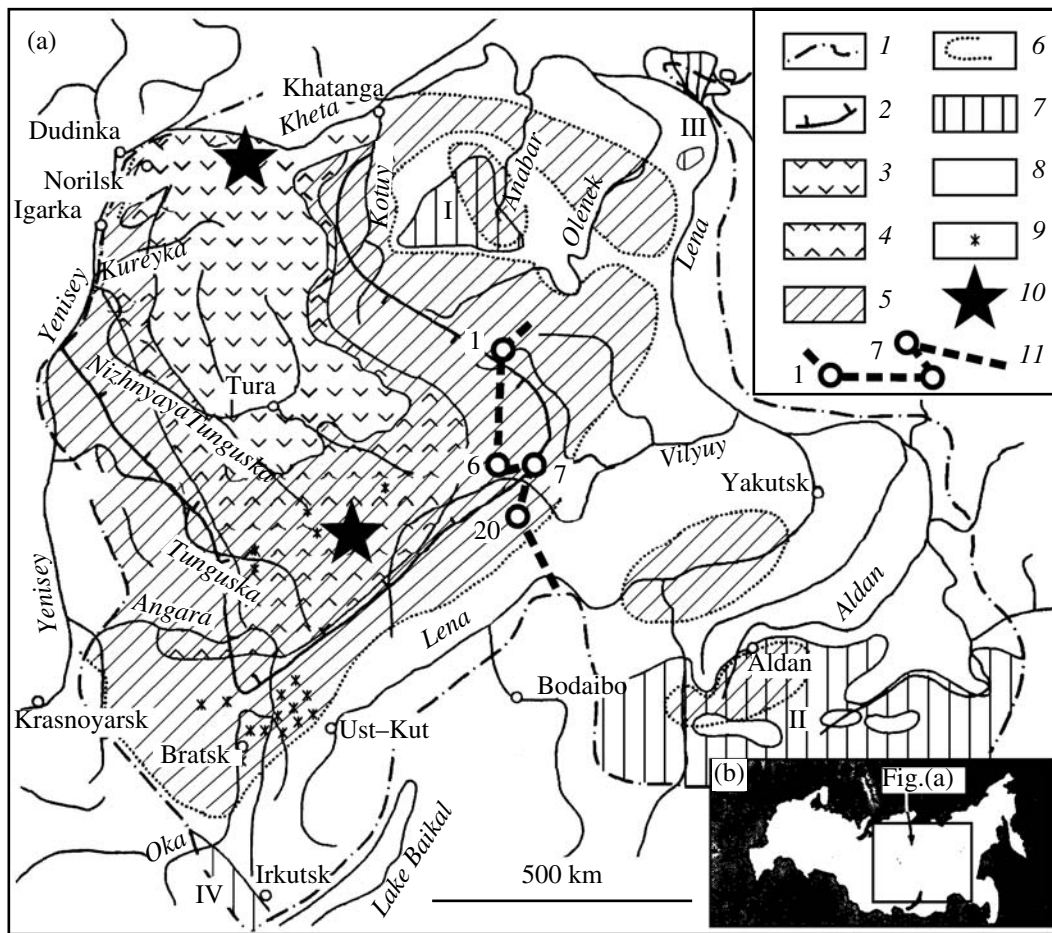


Fig. 10. Sketch map of the Siberian trap province (modified after Fedorenko et al. [1996]). Boundaries of: 1. Siberian platform, 2. Tunguska syncline; Putorana plateau: 3. lavas, 4. tuffs; Sills and dykes: 5. areal extent, 6. limits; 7. basement exposures: I Anabar shield; II Aldan shield; III Olenek uplift; IV Sharyzhalgay uplift; 8. platform cover; 9. basalt pipes; 10. inferred centers of “secondary” mantle plumes [Dobretsov, 1997; Dobretsov et al., 2006]; 11. cross section and location of samples used in this study for AFT dating.

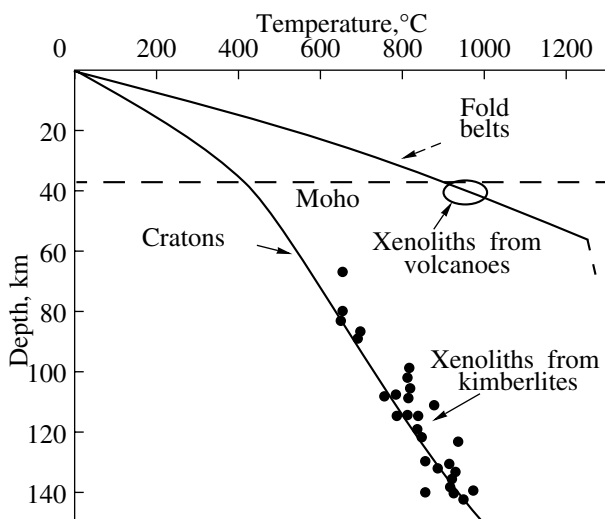


Fig. 11. A temperature against depth plot derived for the fold belts and adjacent cratons [Hyndman et al., 2005].

AFT ages, from 222 to 185 Ma, are interpreted to reflect reversals in magma flow directions and variations in basalt temperatures during the underplating or thermal diffusivity of the rocks in the sections, because the distance between the dated samples range from 200 to 400 km.

Mesozoic plume-derived flood basalts form the so-called Large Igneous Provinces (LIP) in almost all continents within the craton boundaries. A thermal event, similar to the above described, that was induced by basaltic underplating related to Mesozoic plume activity would be manifested in a mature continental crust and within the ancient cratons, in particular, at 100 Ma in Antarctica [Jacobs et al., 1995]. Besides in the Mesozoic, large igneous provinces were formed during the Paleozoic and Proterozoic [Ernst, 2007]. In the light of the presented data, episodes of heating to ~100°C may have occurred within the stable crust of some ancient

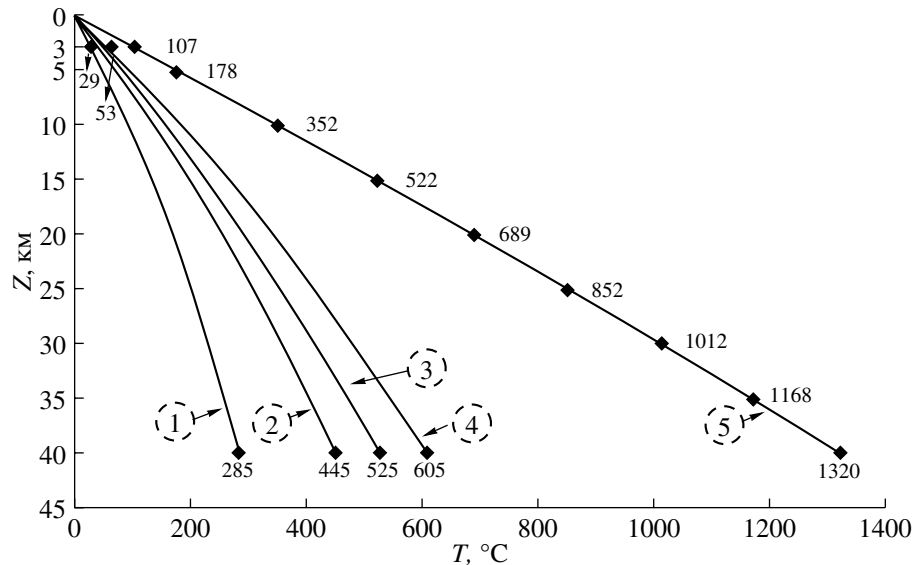


Fig. 12. A temperature (T , °C) against depth (Z , km) plot, characterizing the thermal regime in the crust beneath the Siberian platform in Phanerozoic time.

Geotherms: 1. present time ($Q_0 = 25 \text{ mW/m}^2$); 2–4, during kimberlite emplacement; 2. 360–344 Ma ($Q_0 = 35 \text{ mW/m}^2$); 3. 245–135 Ma, $Q_0 = 40 \text{ mW/m}^2$; 4. probable maximum ($Q_0 = 45 \text{ mW/m}^2$), 5. during basaltic underplating, 250 Ma ago, when the 1320°C basaltic sill was intruded into the base of the crust.

cratons, where flood basalts have formed during the Proterozoic or Paleozoic.

CONCLUSIONS

Modeling the thermal history of the crust of the northeastern Siberian craton enabled us to recognize ten major thermal events, since Archean grey gneiss (TTG) suites until the present time. The studied mineral, apatite, in Archean rocks has been largely overprinted by collision-related metamorphism at 1.8–1.9 Ga. The last recorded thermal event was the self-heating of the collision prism during the accretion of the Siberian craton. This event was terminated by cooling at ~1.3 Ga when the upper crust had passed through the ~300°C isograd and the Rb-Sr biotite systems became closed. The cooling rate was 1.3°C/Ma. The calculation results showed that on further cooling, the ~100°C isograd was passed at 1143 Ma. This value would be obtained by apatite fission-track dating if this thermal event were the last one, as was the case, for example, in Finland where the fission-track dates were estimated to be ≥ 0.8 Ga.

The AFT ages presented here suggest that there existed another, independent thermal event, which significantly post-dated the Early Proterozoic collision. This was probably the Mesozoic plume-related magmatism.

During the Mesozoic flood basalt magmatism (250 Ma) on the Siberian craton, the sills and dykes moved away from vertical feeder conduits, the loci of intrusion of a secondary plume, over 500–1000 km.

The extensive lateral transport of the melt usually occurred along the weak zones and was likely manifested at the base of the crust (basaltic underplating). After the crust was heated through its entire thickness, it began to cool. In the course of cooling, the crust at depths of 2000–3000 m, near the top of the crystalline basement, reached the ~100°C isograd at 222–185 Ma.

The $\geq 100^\circ\text{C}$ heating recorded for the top of the crystalline basement of the Siberian platform may be indicative of the related heating of rocks at the base of the sedimentary cover and thus may help in obtaining the age of the processes of the transformation of organic matter and oil generation.

This finding suggests that similar episodes of underplating and heating of a mature and stable continental crust took place extensively in all continents, where large flood basalt provinces were formed not only in the Mesozoic but also in the Paleozoic and Proterozoic.

ACKNOWLEDGMENTS

This work was supported by grant no. MD-2721.2008.5 from the Russian President, the Program of the Earth Science Division, Russian Academy of Sciences no. 4, National Science Assistance Foundation, and the Russian Foundation for Basic Research (project no. 06-05-64332). The authors take this opportunity to thank E.V. Artyushkov, A.V. Manakov, S.Yu. Milanovskii, and O.P. Polyanskii for their useful discussions. The authors also thank V.P. Serenko and Z.V. Spetsius for their assistance in preparing materials for analyses.

REFERENCES

1. E. V. Artyushkov, *Physical Tectonics* (Nauka, Moscow, 1993) [In Russian].
2. I. V. Ashchepkov, N. P. Pokhilenko, A. M. Logvinova, N. P. Vladykin, A. Ya. Rotman, S. V. Palessky, N. V. Alymova, and E. V. Vishnyakova, "Evolution of Kimberlite Magmatic Sources beneath Siberia" in *Goldschmidt Conference Abstracts A39*, 2007.
3. W. A. Bohron and F. J. Spera, "Energy-Constrained Open-System Magmatic Processes II: Application of Energy-Constrained Assimilation-Fractional Crystallization (EC-AFC) Model to Magmatic Systems," *J. Petrol.* **42**, No.5, 1019–1041 (2001).
4. M. T. Brandon, "Decomposition of Mixed Grain-Age Distributions using BINOMFIT," *On Track*, **24**, 13–18 (2002).
5. M. T. Brandon, "Probability Density Plot for Fission-Track Grain-Age Samples," *Radiation Measurements*, **26**, No. 5, 663–676 (1996).
6. K. Condie, *Plate Tectonics and Crustal Evolution* (Pergamon Press, Oxford, 1989).
7. C. B. Dalrymple, C. K. Czamanske, V. A. Fedorenko, et al., "A Reconnaissance $40\text{Ar}/39\text{Ar}$ Geochronologic Study of the Ore-Bearing and Related Rocks, Siberian Platform, Russia," *Geochem. et Cosmochem. Acta.* **59**, No. 10, 2071–2208 (1995).
8. G. L. Devis, N. V. Sobolev, and A. D. Kharkiv, "New Data on Yakutian Kimberlite Ages Obtained by U-Pb Zircon Dating," *Dokl. Akad. Nauk SSSR* **254**, 175–179 (1980).
9. N. L. Dobretsov, "Permo-Traissic Magmatism and Sedimentation in Eurasia as Manifestation of a Super-Plume," *Dokl. Akad. Nauk SSSR* **354**, No. 2, 220–223 (1997).
10. N. L. Dobretsov, A. A. Kirdyashkin, A. G. Kirdyashkin, et al., "Parameters of Hot Spots and Thermochemical Plumes during Upwelling and Eruption," *Petrologiya*, **14**, No. 5, 508–523 (2006).
11. A. D. Duchkov, V. T. Balobaev and S. V. Lysak, "Heat Flow in Siberia," *Geologiya i Geofizika*, No. 1, 42–51 (1982).
12. A. D. Duchkov and L. S. Sokolova, "Lithospheric Temperature in Siberia by Geothermal Data," *Geologiya i Geofizika*, No.12, 60–71 (1985).
13. A. D. Duchkov and L. S. Sokolova, "Thermal Pattern of the Lithosphere of the Siberian Platform," *Geologiya i Geofizika*, **38**, No. 2, 494–503 (1997).
14. P. C. England and B. Thompson, "Pressure-Temperature-Time Paths of Regional Metamorphism," *Jour. Petrol.* **25** (4), 894–955 (1984).
15. R. E. Ernst, "Mafic-Ultramafic Large Igneous Provinces (LIPs): Importance of the Pre-Mesozoic Record," *Episodes*, **30**, No. 2, 108–114 (2007).
16. V. A. Fedorenko, P. C. Lightfoot, A. J. Naldrett, et al., "Petrogenesis of the Flood-Basalt Sequence at Norilsk, North Central Siberia," *Int. Geol. Review*, **38**, 99–135 (1996).
17. A. J. W. Gleadow, B. P. Kohn, R. W. Brown, P. B. O'Sullivan, and A. Raza, "Fission Track Thermotectonic Imaging of the Australian Continent," *Tectonophysics*, **349**, 5–21 (2002).
18. W. L. Griffin, F. V. Kaminsky, C. G. Ryan, S. Y. O'Reilly, T. T. Win, and I. P. Ilupin, "Thermal State and Composition of the Lithospheric Mantle Beneath the Daldyn Kimberlite Field, Yakutia," *Tectonophysics*, **262**, 19–33 (1996).
19. W. L. Griffin, C. G. Ryan, F. V. Kaminsky, S. Y. O'Reilly, L. M. Natapov, T. T. Win, P. D. Kinney, and I. P. Ilupin, "The Siberian Lithosphere Traverse: Mantle Terranes and the Assembly of the Siberian Craton," *Tectonophysics*, **310**, 1–35 (1999).
20. B. Hendriks, P. Andriessen, Y. Huigen, C. Leighton, T. Redfield, G. Murrell, K. Gallagher, and S. Bom Nielsen, "A fission Track data Compilation for Fennoscandia," *Norwegian Jour. Geol.* **87**, 143–155 (2007).
21. A. J. Hurford, "Zeta: the Ultimate Solution to Fission-Track Analysis Calibration or just an Interim Measure?" in *Advances in Fission-Track Geochronology* (Kluwer Academic Publisher, 1998), pp. 19–32.
22. R. D. Hyndman, C.A. Currie, and S. P. Mazzotti, "Subduction Zone Backarcs, Mobile Belts, and Orogenic Heat," *GSA Today*, **15**, No.2, 4–10 (2005).
23. J. Jacobs, H. Ahrendt, H. Kreutzer, and K. Weber, "K-Ar, 40Ar - 39Ar and Apatite Fission-Track Evidence for Neoproterozoic and Mesozoic Basement Rejuvenation Events in Heimefrontfjella and Mannefallknausane (East Antarctica)," *Precamb. Res.* **75**, 251–262 (1995).
24. J. Jacobs and C. Breikreuz, "Zircon and Apatite Fission-Track Thermochronology of Late Carboniferous Volcanic Rocks of the NE German Basin," *Int. J. Earth. Sci. (Geol Rundsch)*. **92**, 165–172 (2003).
25. R. A. Jamieson, C. Beaumont, P. Fullsack, et al., "Barrovian Regional Metamorphism: Where's the Heat?" in *What Drives Metamorphism and Metamorphic Reactions?* Eds. by P. J. Treloar and P. J. O'Brien (Geol. Soc. London Spec. Publ. **138** 1998), pp. 23–51.
26. P. D. Kinney, B. J. Griffin, L. M. Heamen, et al., "SHRIMP U-Pb Ages of Perovskites," *Geologiya i Geofizika*, **38**, No. 1, 91–99 (1997).
27. S. A. Larson, C. E. Cederbom, E.-L. Tullborg, and J.-P. Stiberg, "Discussion. Comment on "Apatite Fission Track and (U-Th)/He Data from Fennoscandia: An Example of Underestimation of Fission Track Annealing in apatite" by Hendriks and Redfield [Earth Planet. Sci. Lett. 236 (443–158)]," *Earth Planet. Sci.Lett.* **248**, 561–568 (2006).
28. G. M. Laslett, P. F. Green, I. R. Duddy, and A. J. W. Gleadow, "Thermal Annealing of Fission Tracks in Apatite," *Chem. Geol. Isotope Geoscience Section*, **65**, No. 1, 1–13 (1987).
29. M. Lorencak, B. P. Kohn, K. G. Osadetz, and A. J. W. Gleadow, "Combined Apatite Fission Track and (U-Th)/He Thermochronometry in a Slowly Cooled Terrane: Results from a 3440-m-Deep Drill Hole in the Southern Canadian Shield," *Earth Planet Sci. Let.* **227**, 87–104 (2004).
30. A. V. Manakov, *Peculiarities of the Lithosphere Structure of the Yakutian Kimberlite Province* (Voronezh State University, Voronezh, 1999).
31. *Map of Anomalous Magnetic Field of the USSR and Adjacent Territories, Scale 1:10000000* T. P. Litvinova, N. P. Shmiyarova, and L. V. Ermoshko (Map Reprodu-

- tion Plant of Aerogeologiya Association, Leningrad, 1978).
32. *Map of Metamorphic Complexes and Granitoids of the USSR, Scale 1: 10000000*, Ed. by B. Ya. Khoreva (Cartographic enterprise of the Ministry of Geology, Leningrad, 1987).
 33. H. Martin and J.-F. Moyen, "Secular Changes in Tonalite-Trondhjemite-Granodiorite Composition as Aarkers of the Progressive Cooling of Earth," *Geology*, **30**, 319–322 (2002).
 34. G. R. Murrell and P. A. M. Andriessen, "Unravelling a Long-Term Multi-Event Thermal Record in the Cratonic Interior of Southern Finland through Apatite Fission Track Thermochronology," *Physics and Chemistry of the Earth*. 2004. V. 29. P. 695-706 (2004).
 35. O. I. Parfenuk and J.-C. Mareschal, "Therm-Mechanical Model of Evolution of Layered Lithosphere in Continental Collision Zones," XXII EGA General Assembly. *Annales Gaeophysicae*. **15** (1997).
 36. O. I. Parfenuk, Doctoral Dissertation in Mathematics and Physics (Institute of Earth's Physics, Moscow, 2004).
 37. H. N. Pollack and D. S. Chapman, "Mantle Heat Flow," *Earth Planet Sci. Lett.* **34**, 174–184 (1977).
 38. P. R. Renne and A. R. Basu, "Rapid Eruption of the Siberian Traps Flood Basalts at the Permo-Triassic Boundary," *Science*, **253**, 176–179 (1991).
 39. O. M. Rosen and O. M. Turkina, "The Oldest Rock Assemblages of the Siberian Craton," in *Earth's Oldest Rocks. Developments in Precambrian Geology*, Eds. M. J. Van Kranendonk, R. H. Smithies, and V. C. Bennett (Elsevier. Amsterdam-Tokyo, 2007), No. 15, Chap. 6.4, pp. 495–541.
 40. O. M. Rosen, A. V. Manakov, and V. D. Suvorov, "Collisional System of the Northeast of the Siberian Craton and a Problem of the Diamondiferous Lithospheric Keel," *Geotektonika*, No. 6, 1–26 (2005).
 41. O. M. Rosen, "Phanerozoic Mantle Magmatism on the Siberian Platform, Some Constraints on the Mantle Convection Model," *Dokl. Akad. Nauk*, **370**, No.6, 785–788 (2000).
 42. O. M. Rosen, "The Early Precambrian of the East Siberian Platform," *Mineral. Zhurnal (Ukraine)*, Vol. 26, No. 3, 75–87 (2004).
 43. O. M. Rosen, "The Siberian Craton: Tectonic Zonation and Problems of the Evolution," *Geotektonika*, No. 3, 1–19 (2003).
 44. O. M. Rosen, "Heat Generation in the Crust Beneath the Anabar Shield and Problems of the Formation of the Lower Continental Crust," *Geologiya i Geofizika*, No. 12, 22–29 (1992).
 45. O. M. Rosen, A. N. Vishnevskii, M. Z. Glukhovskii, et al., *The Structure of the Earth's Crust Beneath the Anabar Shield* (Nauka, Moscow, 1986) [In Russian].
 46. O. M. Rosen, L. K. Levskii, D. Z. Zhuravlev, et al., "The Paleoproterozoic Accretion in the Northeast of the Siberian Craton: Isotope Dating of the Anabar Collisional System," in *Stratigraphy. Geol. Correlation*, Vol. 14, No.6, 3–24 (2006a).
 47. O. M. Rosen, L. K. Levskii, D. Z. Zhuravlev, et al., "Composition and Age of the Lower Crust in the Northeastern Siberian Platform: a Study of Xenoliths from Kimberlites and Deep Drill Core," *Izv. Vuzov. Geologiya i Razvedka*, No. 4, 18–28 (2006b).
 48. O. M. Rosen, L. K. Levskii, D. Z. Zhuravlev, Z. V. Spetsius, A. Ya. Rotman, N. N. Zinchuk, and A. V. Manakov, "The Anabar Collisional System: a 600-Ma Compression within the Columbia Super-Continent (2.0–1.3 Ga)," *Dokl. Akad. Nauk*, **417**, No. 6, 1–4 (2007).
 49. O. M. Rosen, A. V. Manakov, N. I. Gorev, and N. N. Zinchuk, "Kimberlites, Alkaline Ultramafic Carbonatite-Bearing Complexes and Traps - Different Forms of the Plume Magmatism on the Siberian Craton," in *Problems of Prediction and Exploration of Diamond Deposits within the Closed Territories*, (Izd. YaNC SO RAN, Yakutsk, 2008), pp. 32-37.
 50. O. M. Rosen and S. Yu. Milanovskii, "Geothermal Gradient, Heat Flow and Thickness of the Primary Crust," in *The Archean of the Anabar Shield and Problems of the Early Evolution of the Earth* (Nauka, Moscow, 1988), pp. 203–214.
 51. O. M. Rosen, V. P. Serenko, Z. V. Spetsius, et al., "The Yakutian Kimberlite Province: Position within the Siberian Craton, Specific Features of Composition of the Upper and Lower Crust (Based on Core Data and Inclusions in Kimberlites)," *Geologiya i Geofizika*, **43**, No. 1, 3–26 (2002).
 52. O. M. Rosen and V. S. Fedorovskii, *Collisional Granitoids and Stratification of the Earth Crust* (Nauchnyi Mir, Moscow, 2001) [In Russian].
 53. O. M. Rosen and A. A. Shchipanskii, "Geodynamics of the Early Precambrian. Article 2. Formation of the Continental Crust and Sedimentary Basins, Specific Features of the Lithosphere," in *Stratigraphy. Geol. Correlation*, Vol. 15, No. 6, 3–27 (2007).
 54. R. L. Rudnick and S. Gao, "Composition of the Continental Crust," in *Treatise on Geochemistry*. Eds. H. D. Holland and K. K. Turekian (Elsevier, Amsterdam, 2003), Vol. 3.01, pp. 1–64.
 55. R. L. Rudnick and D. M. Fountain "Nature and Composition of the Continental Crust: a Lower Crustal Perspective," *Rev. Geoph.* **33**, No. 3, 267–309 (1995).
 56. J. Siivola and R. Schmid, "List of Mineral Abbreviations," in *Metamorphic Rocks: A Classification and Glossary of Terms* Eds. D. Fettes and J. Desmons (Cambridge University Press. Cambridge UK, 2007), Chap. 2.12, pp. 93-110.
 57. A. P. Smelov, V. P. Kovach, V. D. Gabyshev, et al., "Tectonic Structure and Age of the Basement in the Northeastern Part of the North Asian Craton," *Otechest. Geologiya*, No. 6, 6–10 (1998).
 58. A. V. Soloviev, "A Study of the Tectonic Processes in Areas of the Lithospheric Plate Convergence: Methods of Track and Structural Analyses," in *Transactions of Geol. Institute* (Moscow, Nauka, 2008), **577**.
 59. M. Thoni, "Sm-Nd Isotope Systematics in Garnet from Different Lithologies (Eastern Alps): Age Results, and an Evaluation of Potential Problems for Garnet Sm-Nd Chronometry (Erratum)," *Chemical Geology*, **194**, 353–379 (2003).
 60. A. N. Vishnevskii, Doctoral Dissertation in Geology and Mineralogy (PGO Sevmorgeologiya, Leningrad, 1988).
 61. G. A. Wagner and P. Van den Haute, *Fission-Track Dating* (Kluwer Academic Publishers. Dordrecht, 1992).